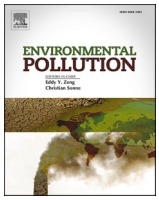
Environmental Pollution 355 (2024) 124217



Contents lists available at ScienceDirect

Environmental Pollution

journal homepage: www.elsevier.com/locate/envpol





Assessment of biodegradation and toxicity of alternative plasticizer di (2-ethylhexyl) terephthalate: Impacts on microbial biofilms, metabolism, and reactive oxygen species-mediated stress response☆

Dana Fahad M.S. Mohamed [a], Abhrajyoti Tarafdar [a,b], So Yeon Lee [c], Han Bin Oh [c], Jung-Hwan Kwon [a,*]

[a] Division of Environmental Science and Ecological Engineering, Korea University, Seongbuk-gu, Seoul, 02841, Republic of Korea
[b] School of Food Science and Environmental Health, Technological University Dublin, City Campus, Grangegorman, Dublin, D07ADY7, Ireland
[c] Department of Chemistry, Sogang University, Seoul, 04107, Republic of Korea

ARTICLE INFO

Keywords:
Biofilm
Biodegradation
Carboxylation
DOTP
Hydrolyzation
Microplastics

ABSTRACT

Although di(2-ethylhexyl) terephthalate (DOTP) is being widely adopted as a non-phthalate plasticizer, existing research primarily focuses on human and rat toxicity. This leaves a significant gap in our understanding of their impact on microbial communities. This study assessed the biodegradation and toxicity of DOTP on microbes, focusing on its impact on biofilms and microbial metabolism using *Rhodococcus ruber* as a representative bacterial strain. DOTP is commonly found in mass fractions between 0.6 and 20% v/v in various soft plastic products. This study used polyvinyl chloride films (PVC) with varying DOTP concentrations (range 1–10% v/v) as a surface for analysis of biofilm growth. Cell viability and bacterial stress responses were tested using LIVE/DEAD™ BacLight™ Bacterial Viability Kit and by the detection of reactive oxygen species using CellROX™ Green Reagent, respectively. An increase in the volume of dead cells (in the plastisphere biofilm) was observed with increasing DOTP concentrations in experiments using PVC films, indicating the potential negative impact of DOTP on microbial communities. Even at a relatively low concentration of DOTP (1%), signs of stress in the microbes were noticed, while concentrations above 5% compromised their ability to survive. This research provides a new understanding of the environmental impacts of alternative plasticizers, prompting the need for additional research into their wider effects on both the environment and human health.

1. Introduction

Diverse additives are used to improve the physical, mechanical, and chemical properties of plastic products (Beach et al., 2013; Bolívar-Subirats et al., 2021). One commonly used type of additive is phthalate plasticizers, such as diethylhexyl phthalate (DEHP), which have been widely employed for many years to enhance the flexibility, durability, and workability of polyvinyl chloride (PVC) (Rais-Bahrami et al., 2004; Latini et al., 2010; Chiellini et al., 2013; Bodaghi, 2019). However, there are growing concerns regarding the potential adverse health effects and environmental impact of phthalates, particularly their association with endocrine disruption (Meeker et al., 2009; Kumar, 2018; Darbre, 2020; Pérez-Albaladejo et al., 2020). The European Union classifies DEHP as a substance of high concern (SVHC) under the REACH and Toy Safety Directives and prohibits its usage in toys and baby care items (Unterberg et al., 2011; Lorenzetti et al., 2015). The Consumer Product Safety Improvement Act in the United States (CPSIA) forbids DEHP and other phthalates in infant and children's products (Shah and Burgess, 2009; Boor et al., 2015). Similar restrictions apply to DEHP in toys and baby products in Canada under the Environmental Protection Act (CEPA) (Eichler et al., 2019). These regulations have prompted the search for safer alternatives of DEHP in many consumer products (Kim et al., 2020).

In response to these concerns, di(2-ethylhexyl) terephthalate (DOTP) emerged as a viable substitute for traditional phthalate plasticizers (Harmon and Otter, 2018). It is a non-*ortho*-phthalate plasticizer that

Abbreviations: DOTP, Di(2-ethylhexyl) terephthalate; *R. ruber*, *Rhodococcus ruber*; PVC, Polyvinyl Chloride; ROS, Reactive Oxygen Species.

☆ This paper has been recommended for acceptance by Yucheng Feng.

* Corresponding author.
E-mail address: junghwankwon@korea.ac.kr (J.-H. Kwon).

https://doi.org/10.1016/j.envpol.2024.124217
Received 21 January 2024; Received in revised form 4 May 2024; Accepted 23 May 2024
Available online 24 May 2024
0269-7491/© 2024 Elsevier Ltd. All rights are reserved, including those for text and data mining, AI training, and similar technologies.

was introduced as an alternative capable of delivering performance comparable to traditional options (Krauskopf, 2003). DOTP exhibits a higher molecular weight and lower volatility compared to phthalates, leading to improved stability and reduced migration from plastic products (Tüzüm Demir and Ulutan, 2013, 2015). DOTP is typically found in soft plastic products in chemical mass fractions within the range of 0.6%–20% (Xie et al., 2016; Aurisano et al., 2021). This attribute is particularly crucial in applications involving direct human contact or exposure to food and beverages (Harmon and Otter, 2022; Kim et al., 2022).

The industry embraced DOTP as a safer alternative to phthalate plasticizers. Consequently, recent studies have found DOTP dominant in coastal sediments, with notable occurrences reported in Korea and Tunisia (Lee et al., 2020; Kim et al., 2021; Jebara et al., 2021). This suggests widespread contamination of the coastal environment. Furthermore, there is limited research on the biodegradation of DOTP. Earlier investigations involving *Rhodococcus rhodochrous* demonstrated that plasticizers such as di-ethylhexyl adipate (DEHA), dioctyl phthalate (DOP), and DOTP did not undergo degradation in the absence of an additional carbon source, such as hexadecane (Nalli et al., 2002). In this study, we deemed it important to investigate the biodegradation of DOTP by bacterial species known for their ability to degrade plastics.

Rhodococcus ruber is a Gram-positive, aerobic, non-spore-forming bacterial species that is commonly found in diverse environmental settings (Guevara et al., 2019). It has been isolated from various habitats, including soil, freshwater, marine environments, and even extreme conditions like hot springs and oil-contaminated areas (Yang et al., 2018; Goudriaan et al., 2023). The versatility of *R. ruber* in terms of biological distribution has drawn considerable attention in the field of plastic degradation (Gilan and Sivan, 2013; Auta, 2017; Pathak and Navneet, 2017). This bacterium possesses the capability to metabolize and break down a wide range of synthetic polymers (Sharma and Neelam, 2023), including polyethylene terephthalate (PET), polyethylene (PE), polystyrene (PS), and polyurethane (PU) (Mor and Sivan, 2008; Krivoruchko et al., 2018; Ghatge et al., 2020; Naloka et al., 2022). The enzymes produced by *R. ruber* act on these plastics, breaking them down into smaller molecules that can be utilized by this bacterium as a source of carbon and energy (Sharma and Neelam, 2023). Understanding the interactions between *R. ruber* and plastics, as well as the potential degradation of plastic additives by microbes, is crucial in comprehending the breakdown and degradation processes of various substances in the environment.

Considering the toxicity of plasticizers to microbes is crucial as it can significantly impact natural biodegradation processes (Horn et al., 2004; Ahmad et al., 2022; Tarafdar et al., 2023), disrupt microbial communities (Cartwright et al., 2000; Luo et al., 2022), and cause ecotoxicity (Vikhareva et al., 2021; Tarafdar et al., 2022), leading to ecosystem deterioration. Reactive oxygen species (ROS) form in bacteria via metabolic processes (Seixas et al., 2021), environmental interactions (Morris et al., 2022), and stress responses (Schieber and Chandel, 2014). For example, hydroxyl radicals, representative species of ROS, can destroy nucleic acids, cause protein carbonylation, and peroxidize lipids, leading to cell death if they are not controlled (Imlay, 2013). Thus, understanding ROS levels is important to comprehend how bacteria respond to environmental stress (Zhao and Drlica, 2014; Hong et al., 2019).

This study addresses a critical knowledge gap in understanding the environmental impact of a relatively low-toxicity alternative plasticizer, DOTP. The biodegradation pathway, viability of *R. ruber* in the presence of DOTP, and toxicity of DOTP through the release of ROS were observed. The biodegradation pathway was determined through the utilization of LTQ Orbitrap XL and 15T Fourier-transform ion cyclotrone resonance mass spectrometry (FT-ICR MS) techniques. The elucidation of the biodegradation pathway has, for the first time, offered valuable insights into the environmental fate of DOTP, shedding light on its persistence. The use of specialized dyes to distinguish live and dead cells based on membrane integrity and to gauge cellular toxicity via ROS levels contributes to a holistic understanding of how DOTP might impact microbial communities that inhabit the plastisphere. This investigation provides new insights into the potential impact of DOTP within the plastisphere and microbial communities from alternative environmental compartments, addressing a crucial issue in contemporary environmental research.

2. Materials and methods

2.1. Materials

Rhodococcus ruber strain KCCM 41053 (T) was obtained from Korean Culture Center Microorganisms (Seoul, Republic of Korea). DOTP and PVC (Product no. 81388, molecular weight ~48000) were purchased from Sigma Aldrich (St. Louis, MO, USA). The Bushnell-Haas broth, sourced from HiMedia (Mumbai, India), is a composition of various ingredients in deionized water. It contains 1 g each of K_2HPO_4, KH_2PO_4, and NH_4NO_3, as well as 0.02 g of $CaCl_2$, 0.20 g of $MgSO_4$, and 0.05 g of $FeCl_3$ per liter. The pH of the broth was adjusted to 7 using NaOH (Tarafdar et al., 2021). This carbon-free mineral salt medium was used for microbial enrichment, biodegradation, and biofilm growth. The media was passed through a solid-phase extraction (SPE) cartridge (Oasis HLB, Waters, Milford, MA, USA). Luria Bertani (LB) broth (Sigma-Aldrich, St. Louis, MO, USA) was used as the growth medium. HPLC grade *n*-hexane (≥97.0%, Sigma Aldrich, St. Louis, MO, USA) was utilized for sample preparation, and tetrahydrofuran (≥99.9%, Sigma Aldrich, St. Louis, MO, USA) was used for the preparation of PVC solution. The diagnostic system was run using Milli-Q water.

The LIVE/DEAD™ BacLight™ Bacterial Viability Kit (product no. L13152) and CellROX™ Green Reagent (product no. C10444) dyes were acquired from Invitrogen™ (Waltham, MA, USA) for the purpose of assessing cell viability and quantifying oxidative stress. Additionally, Hoechst 33342 (product no. B2261) was obtained from Sigma-Aldrich.

2.2. Live/dead cell study of R. ruber in an aqueous medium with 0.1% DOTP (v/v)

To investigate the impact of DOTP on *R. ruber* under optimal growth conditions, a volume of 250 mL of sterile LB broth was incubated at 30 °C with continuous shaking at 120 rpm. This temperature mimics the bacterium's ideal environment for growth, allowing us to specifically focus on understanding how DOTP influences its behavior. The samples were incubated in dark conditions to prevent any potential photooxidation effects that could influence the results. Following an incubation period of 24 h, a 1 mL aliquot of the mother culture was taken for subsequent inoculation. The aliquot was subjected to centrifugation at 3000 rpm for 5 min, the supernatant was carefully discarded, and the bacterial cell pellet was then resuspended in 1 mL of sterile milliQ water to eliminate any remaining culture medium components. MilliQ water was used for resuspension to minimize potential interference with subsequent microscopic analysis using CLSM and fluorescent dyes. Finally, the resuspended cells were added to 250 mL of sterile Bushnell Haas broth to determine the growth cycle in the presence of DOTP as the only carbon source.

The Live/Dead BacLight Bacterial Viability Kit L13152 was used to stain the bacteria centrifuged out of the media following the manufacturer's instructions. Propidium iodide, a red fluorescent nucleic acid stain, and SYTO9, a green fluorescent nucleic acid stain, are both included in the kit. These stains differ in terms of both their spectral properties and capacity to enter healthy bacterial cells depending on their membrane integrity. To rule out any false positive results, media without bacteria (negative control) were also stained. They were dried in the dark for 20 min and analyzed using confocal laser scanning microscopy (CLSM). To capture images, a Zeiss LSM 700 AxioObserver CLSM was utilized alongside Zeiss Zen 2012 software from Carl Zeiss

(Oberkochen, Germany). Image acquisition was carried out using a Plan-Apochromat objective with a magnification of 10 × and a numerical aperture of 0.45. The captured digital images had dimensions of 512 × 512 pixels, covering an area of 1.28 × 1.28 mm, and were encoded with 8 bits per pixel. The cover glass thickness was measured to be 0.17 mm. The experimental procedure involved staining cells with SYTO 9 and propidium iodide, which have specific excitation/emission maxima at 480/500 nm and 490/635 nm, respectively. The setup included an MBS 405/488/555/639 beam splitter and a photon multiplier tube detector. To reduce noise and improve visibility, the gain/intensities were adjusted for the green, red, and blue channels. Once the CLSM adjustment settings were optimized, they remained consistent for all scans conducted during the experiment. Volumetric measurements were obtained by capturing a Z-stack series, where consecutive slices were taken at distances of 5 and 7 μm. Each image in the series comprised 15-22 slices (i.e., focal planes). To visualize the three-dimensional information in a two-dimensional format, orthogonal projection with maximum intensity was employed to flatten the image. The live/dead ratio was determined using ImageJ software, specifically the Color Pixel Counter plugin (National Institute of Health, Bethesda, MR, USA).

2.3. Biodegradation of DOTP and detection of degradation metabolites using mass spectrometry

A concentration of 0.1% v/v DOTP was selected for this study, aligning with the concentrations commonly employed in other biodegradation studies of plasticizers (Wright et al., 2020). Sterilized Bushnell Haas broth (250 mL) was prepared to contain *R. ruber* and 0.1% v/v DOTP. DOTP is not dissolved into the sample directly. DOTP is incrementally added in was shaken at 120 rpm and 30 °C in a shaking incubator. Samples were extracted at 36 h and 72 h. Biodegradation at 36 h was observed to unveil potential early-stage metabolites and intermediates that could be found in the biodegradation process. Simultaneously, the extended 72 h duration allows for the examination of metabolites found over a longer period, offering insights into potential late-stage metabolites and the overall progression of biodegradation. A control sample (250 mL) was made using the same conditions, containing only *R. ruber* and no DOTP. After each time interval, the samples were filtered through a glass microfiber filter (pore size 1.5 μm, Whatman, UK) to separate any debris from the medium. The solid-phase extraction (SPE) cartridge (Oasis HLB 6 cc Vac Cartridge, 200 mg Sorbent per Cartridge, 30 μm, Waters Corporation, Milford, MA, USA) was initially pre-conditioned with MilliQ water to ensure optimal performance. The filtrate underwent centrifugation at 3000 rpm for 10 min to separate any remaining bacterial cells from the liquid medium. Subsequently, the liquid medium passed through the SPE cartridge to capture retained metabolites. These metabolites were then eluted from the SPE cartridge using 10 mL of hexane. The efficiency of the extraction process was further validated by the inclusion of known concentrations of DOTP in control samples. Regular checks on the performance of the SPE cartridge, including the flow rate and elution efficiency, were conducted to maintain consistent and reliable recovery rates. For mass spectrometric profiling, the samples were initially analyzed with gas chromatography-mass spectrometry (GC-MS), then with LTQ Orbitrap XL (ThermoFisher Scientific, Waltham, MA, USA) and 15T FT-ICR MS (Bruker Daltonics SolariX (MS:1001549), MA, USA).

Agilent 7890A gas chromatograph (GC) equipped with a 5975C mass spectrometry detector (MSD) from Agilent Technologies (Santa Clara, CA, USA) was used. Separation was achieved using an Agilent DB-5MS capillary column measuring 30 m in length and 0.25 mm in diameter, with a film thickness of 0.35 μm. Helium was the carrier gas and maintained at a constant flow rate of 1 mL min^{-1}. The inlet temperature was set to 300 °C, with a pressure of 10.52 psi. The GC oven temperature was initially set to 100 °C and then ramped up at a rate of 15 °C per min for 6.67 min until it reached 200 °C. Subsequently, the temperature increased at a rate of 5 °C/min until it reached 270 °C. The total runtime for each sample was 36.67 min. The ions were monitored using both scan mode and selective ion monitoring mode. To quantify the concentration of DOTP, benzyl benzoate was employed as an internal standard. External standards were prepared with concentrations ranging from 0.1 μg mL^{-1} to 100 μg mL^{-1}. The mass-to-charge ratios (m/z) selected were 149 and 167 for DOTP, and 212 and 213 for benzyl benzoate, respectively The calibration curve exhibited a high coefficient of determination ($R^2 = 0.99$), indicating a strong linear correlation between DOTP concentrations and instrument response. To evaluate the absence of analyte carry-over in the GC-MS system, hexane was injected as a control between each analysis of the samples.

For the Orbitrap analysis, the solvent from each sample was dried and then dissolved in methanol. The atmospheric pressure chemical ionization (APCI) source was operated in both positive and negative modes within a mass range of m/z 50–500. In both modes, the capillary temperature was maintained at 275 °C, with sheath gas and auxiliary gas flows set at 10 arbitrary units (a. u.) and 5 a. u., respectively. In the positive mode, the tube lens offset voltage and capillary voltages were adjusted to +30 V and +3.0 kV, respectively. In the negative mode, these values were set to −125 V and −2.0 kV, respectively. To enhance the signal-to-noise ratio, multiple scans were performed, and the obtained spectra were averaged. Specifically, 20–30 scanned spectra were acquired and subsequently averaged to obtain representative spectra.

Prior to FT-ICR MS analysis, the instrument was externally calibrated using a sodium trifluoroacetate covering a m/z range from 200 to 1200. To ensure better alignment with theoretical values, internal calibration was performed. For internal calibration, A 600 μL aliquot of each sample was mixed with 360 μL of a positive internal calibration mixture, which included 10 μM 9-phenyl anthracene (100 μL) and 1 μM 9,10-di(1-naphthyl) anthracene (150 μL) in toluene (450 μL). Additionally, 40 μL of a negative internal calibration mixture was added, composed of 10 μM 9-anthracenecarboxylic acid (150 μL), 10 μM heptadecanoic acid (60 μL), and 10 μM stearic acid (120 μL) in methanol (80 μL). The prepared samples were evaporated and reconstituted in methanol. They were then directly infused into an atmospheric pressure photoionization (APPI) source for positive mode and an electrospray ionization (ESI) source for negative mode, covering a mass range of m/z 150–850. The accumulation time was consistently set at 0.1 s, and 200 scans were collected for each sample. For the APPI (+) mode, the settings were as follows: nitrogen nebulizer gas pressure, 1.5 bar; vaporizer temperature, 400 °C; dry temperature 220 °C; drying gas flow rate 4 L min^{-1} and a flow rate of 360 μL h^{-1} with a syringe pump. The following ESI (−) conditions were used: nitrogen nebulizer gas pressure, 0.5 bar; capillary voltage, 3.5 kV; dry temperature 180 °C; drying gas flow rate 4 L min^{-1} and flow rate of 120 μL h^{-1} with a syringe pump. Data analysis software 4.1 (Bruker Daltonics) was utilized for peak identification and internal calibration. Peak lists were established from the raw data when the signal-to-noise ratio exceeded 10. The achieved internal calibration mass accuracy was below 0.5 ppm.

2.4. Preparation of PVC films with DOTP as an additive

PVC films were prepared according to the method reported by Yousif et al. (2015). A solution of PVC (0.05 g mL^{-1}) in tetrahydrofuran was employed to manufacture polymer films. DOTP was added at different concentrations (1, 5, and 10% v/v). The films were created over 24 h at room temperature using an evaporation process inside a laminar flow cabinet to minimize any chance of airborne contaminations. To remove the remaining solvent, the film samples were dried overnight at room temperature. This drying period allowed sufficient time for the solvent to evaporate completely, leaving behind a plastic film. The films were cut into 3 × 3 mm and had a thickness of 0.03 mm. The scanning electron microscope (SEM) images of the surface of PVC films with and without DOTP can be found in Figure S1 (Supplementary Material).

2.5. Live/dead study of R. ruber on the surface of DOTP-infused PVC

A freshly prepared 250 mL LB broth was subjected to inoculation with *R. ruber*. 0.1 g of pristine PVC film (utilized as the control) and PVC film incorporating varying volume fractions of DOTP (1%, 5%, and 10% v/v) were separately introduced into flasks. The cultures were incubated at 30 °C and shaken at 120 rpm for 5 d. A volume of 50 mL LB broth was supplied every 24 h to provide a fresh carbon source. Fresh biofilms on PVC were collected and incubated in the dark with BacLight fluorescent stains for 20 min at room temperature. To eliminate the remaining unbound dye, samples were cleaned with a phosphate buffer solution. The samples were stained, placed on 35 mm glass bottom confocal dish, and analyzed with CLSM. Images in red and green were produced by fluorescence microscopy. The colors red and green stand represent live and dead cells, respectively.

2.6. Toxicity study using CellROX™ green reagent

ROS was used as an indicator for stress caused by DOTP using CellROX™ Green reagent. Being cell-permeable, CellROX™ Green can easily infiltrate bacterial cells. Once within the cell, it is subjected to ROS oxidation, which results in the production of a highly luminous product. Fluorescence microscopy or flow cytometry can be used to identify and measure this fluorescence, giving a reading on the ROS levels present in the bacterial cells. The level of ROS in the cells directly correlates with the strength of the CellROX™ Green fluorescence signal. Increased ROS fluorescence by CellROX™ Green signifies elevated ROS levels, whereas decreased fluorescence shows decreased ROS levels (Wang et al., 2017).

The experiment was conducted in the same way as the live/dead study where 0.1 g of pristine PVC film and varying mass fractions of DOTP (pristine, 1, 5, and 10% v/v) were added to separate flasks and incubated with *R. ruber* for 5 d at 30 °C with continuous shaking at 120 rpm. The staining technique used in this study followed a similar approach as a previous investigation that examined the development of biofilm on the surface of LDPE fibers (Tarafdar et al., 2022). Fresh biofilms formed on PVC films were stained with 5 μL of CellROX™ Green reagent (ex/em: 485/520) and incubated at 37 °C in the dark for 30 min. CellROX™ dyes have been specifically developed to enter living cells and undergo oxidation in the presence of ROS. In their reduced state, the dyes do not emit fluorescence. However, upon oxidation, they exhibit a significant increase in fluorescence intensity (Lozoya-Gloria et al., 2017). Prior to microscopy, the PVC films were cleaned in phosphate-buffered saline (PBS), stained with 1 μg mL^{-1} of Hoescht 33342 (ex/em: 340/510 nm), and incubated for 15 min in the dark. The cell-permeable DNA stain, Hoechst 33342 (2'-[4-ethoxyphenyl]-5-[4-methyl-1-piperidine]), exhibits an affinity for AT-rich regions within the minor groove of double-stranded DNA. Cells stained with Hoechst 33342 were used to identify and enumerate all cells present on the PVC film, including those that are not stressed. In this configuration, stressed cells appeared green (CellROX™ Green), while non-stressed cells appeared blue (Hoescht 33342). In the same excitation and emission range, the autofluorescence of control devoid of CellROX™ Green was examined. The samples were placed on a 35 mm glass-bottom confocal dish and microscopic images were recorded as a Z-stack series using Zeiss LSM 700 AxioObserver CLSM.

2.7. Microscopic analysis and image processing

A field emission scanning electron microscope (FE SEM) (JSM-7500F, Jeol, Tokyo, Japan) was used to examine the surface of the plastic films as well as the morphology of the biofilm growing on the surface of the film. Micro-slides of biofilms were prepared using 2.5% glutaraldehyde in PBS (pH 7). Then, employing solutions containing 50, 75, 90, and 100% ethanol, serial dehydration with increasing ethanol contents was carried out (10 min incubation time). A semi-in-lens detector and a low-intensity electron beam were used to assess the specimens after they had been coated with platinum to improve their visibility in high vacuum conditions. The slides were examined at an accelerating voltage of 5 kV with magnifications ranging from 250 × to 550 × . To observe the plastic surface and bacterial development, the working distance was adjusted to 12.2 mm and 6 mm, respectively.

The BiofilmQ software version 0.2.2 (Drescher lab, Max Planck Institute for Terrestrial Microbiology, Marburg, Germany) was employed to estimate the volume of the biofilms. This was achieved through threshold-based 3D segmentation of confocal images. The CLSM instrument produced image files in the '.czi' format, which were analyzed using BiofilmQ software. The software performed multiple image processing steps to reduce noise and eliminate unwanted fluorescence. These steps included denoising through convolution and background removal and elimination of intercellular fluorescence using Top-Hat filtering. Ridler-Calvard with a sensitivity value of 0.04 was used as the thresholding method. The cube dissection method with a cube side length of 20 was used for object declumping. The total biofilm volume was quantified by selecting global biofilm volume as a parameter to assess variations among different samples. Percentage differences in specific endpoints were computed using mean values derived from triplicate studies of the same sample.

3. Results and discussion

3.1. Live/dead cell study of R. ruber in an aqueous medium with 0.1% DOTP

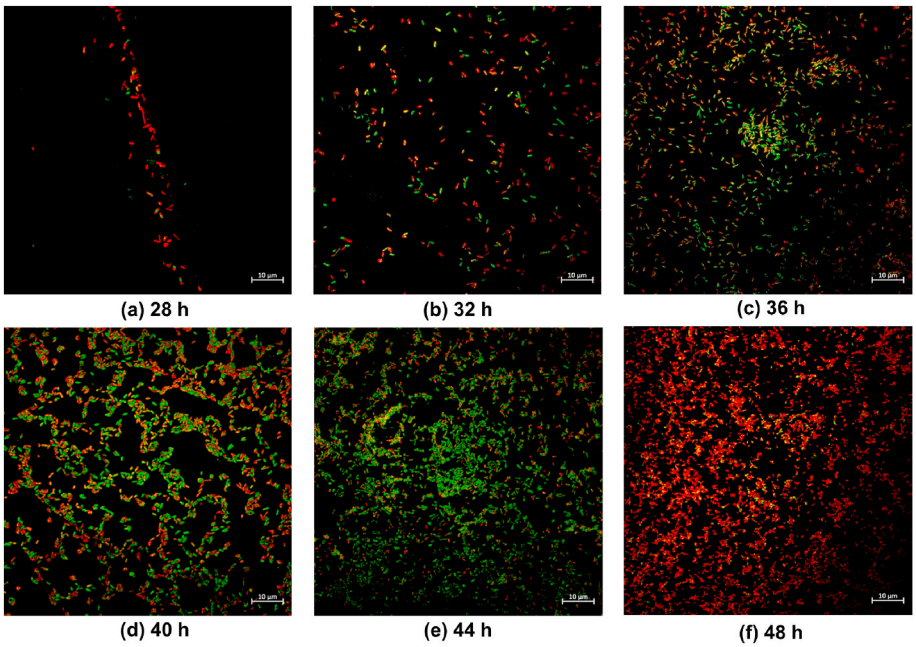
R. ruber was cultured in a carbon-free Bushnell Haas medium to determine the growth cycle when DOTP is provided as the only carbon source. Fig. 1 depicts the amount of bacterial cells collected from the media at different times after incubation. The bacterial cells started to grow at 28 h (Fig. 1a) and the cell biomass gradually increased. The biovolume of live cells was highest at 44 h (Fig. 1e) and the overall biovolume (live and dead) was at its highest at 48 h (Fig. 1f). At 44 h, the ratio based on the average of the collected data is around 1.14 indicating a slight predominance of live cells over dead cells. The predominance of green fluorescence in the 2D image can be attributed to live cells growing over dead cells within the biofilm. After 48 h, the cell population had reached the death phase, indicating a higher number of deceased cells compared to viable cells. (Fig. 1g). This shows that this bacterium can thrive even when DOTP is present as the only carbon source. In the control sample devoid of DOTP, the absence of any observable bacterial growth was attributed to the lack of a carbon source in the sample.

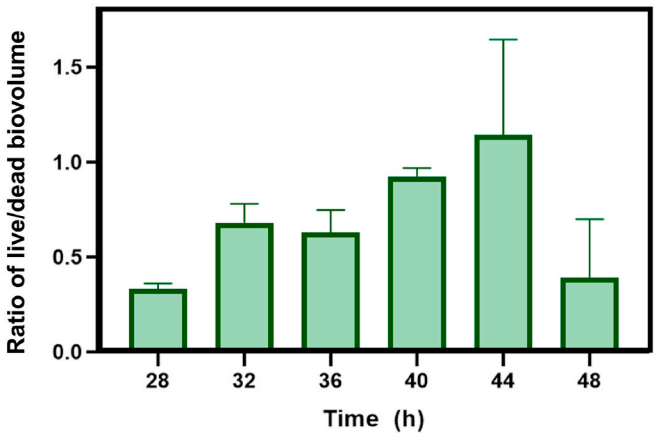
3.2. Biodegradation of DOTP

To investigate the biodegradation pathway of DOTP using the bacterium *R. ruber*, the study employed gas chromatography-mass spectrometry (GC-MS) to detect and identify intermediates produced during the degradation process. Benzoic acid was the most abundant metabolite found with GC-MS analysis. To gain a more comprehensive understanding of the degradation pathway, further investigations were conducted using LTQ Orbitrap XL and 15T FT-ICR MS techniques.

In the Orbitrap analysis, both monoethylhexyl terephthalate and terephthalic acid were detected in samples incubated for 36 and 72 h, specifically when analyzed in positive mode. Moreover, in the 36 h sample analyzed in negative mode, monoethylhexyl terephthalate and benzoic acid were identified. The FT-ICR analysis also confirmed the presence of these metabolites, except for benzoic acid (Fig. S2, Supplementary Material). The absence of benzoic acid detection in the FT-ICR analysis can be attributed to its inherent mass range which starts from 150 m/z.

However, the Orbitrap analysis detected benzoic acid within the mass range of 50–500 m/z at 36 h. This pathway closely corresponds to previously published findings regarding the degradation pathway of





(g) Live/Dead biovolume ratio of *R.ruber* at different time intervals

Fig. 1. (a–f) Growth of *R.ruber* in Bushnell Haas media with DOTP as the only carbon source observed from 28 h to 48 h. **(g)** The ratio of live and dead biovolume observed periodically using ImageJ Color Pixel Counter. Bars represent the mean values of the triplicate Live/Dead cell ratio and the error bars represent the standard deviations. (For interpretation of the references to color in this figure legend, the reader is referred to the Web version of this article.)

DEHP (Yang et al., 2018). The biodegradation of DOTP proceeded through a series of hydrolysis reactions. Initial hydrolysis of DOTP generated monoethylhexyl terephthalates. Hydrolysis, involving the reaction of DOTP with water, facilitated the cleavage of chemical bonds within the DOTP molecule. Subsequent hydrolysis of this intermediate yielded terephthalic acid. Terephthalic acid underwent decarboxylation, involving the removal of a carboxyl group, resulting in the formation of benzoic acid (Fig. 2.). These smaller compounds, such as terephthalic acid and benzoic acid, are more accessible and can be assimilated into the metabolic processes of organisms like *R. ruber*. This elucidation of the biochemical reactions provides a clearer understanding of the transformation of DOTP into components readily utilized in the cellular processes of the bacterium.

3.3. Live/dead study of R. ruber on the surface of DOTP-infused PVC film

Fig. 3 indicates the biovolume after 5 d of incubation. When pristine PVC was examined, the biovolume displayed a higher percentage of live cells (54%) compared to dead cells (46%), with live cells measuring 9054 μm^3 and dead cells measuring 7475 μm^3. However, in the presence of 1% v/v DOTP, the total volume of cells was lower and there were 107% more dead cells (3592 μm^3) present in comparison to live cells (1738 μm^3). This indicates that even at a low concentration in PVC, DOTP appears to affect overall bacterial growth making it difficult for the bacteria to thrive in this environment.

The trend was similar in the sample with a DOTP volume fraction of 5% v/v, however, the total volume of cells was higher (11377 μm^3) than 1% v/v DOTP concentration. DOTP-induced oxidative stress likely contributes to increased bacterial cell density and biofilm growth via quorum sensing, a chemical communication system. Quorum sensing enables bacteria to coordinate activities, such as nutrient acquisition, motility, compounded production and horizontal gene transfer. (Decho, Norman and Visscher, 2010; Mukherjee and Bassler, 2019). Bacteria with quorum sensing survive better under oxidative stress, making it important for biofilm formation and strength (Tarafdar et al., 2022). The sample with 10% v/v DOTP demonstrated the highest cell volume (29154 μm^3) among the tested conditions. However, no live cells were detected in this sample. This suggests that the presence of 10% v/v

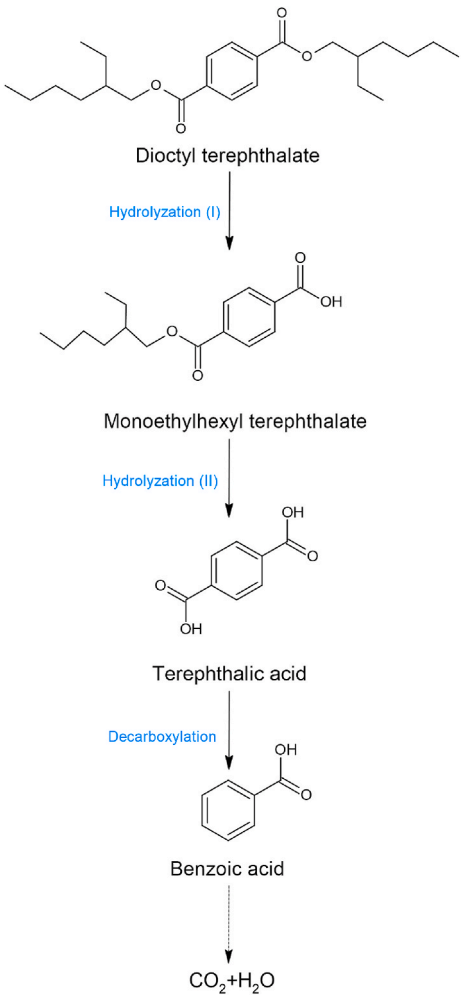


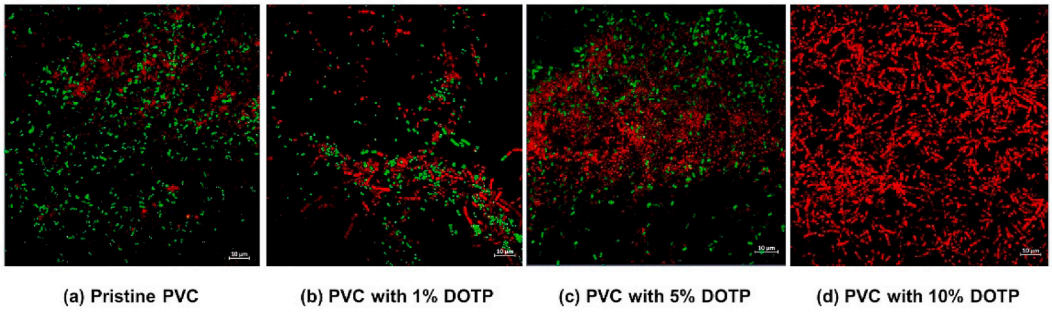
Fig. 2. The proposed degradation pathway of DOTP involves hydrolysis to terephthalic acid, with monoethylhexyl terephthalate as an intermediate. Benzoic acid was also metabolized through the benzoate metabolism for cell growth.

DOTP on the PVC surface had a detrimental effect on the viability of the bacteria, leading to a complete absence of live cells.

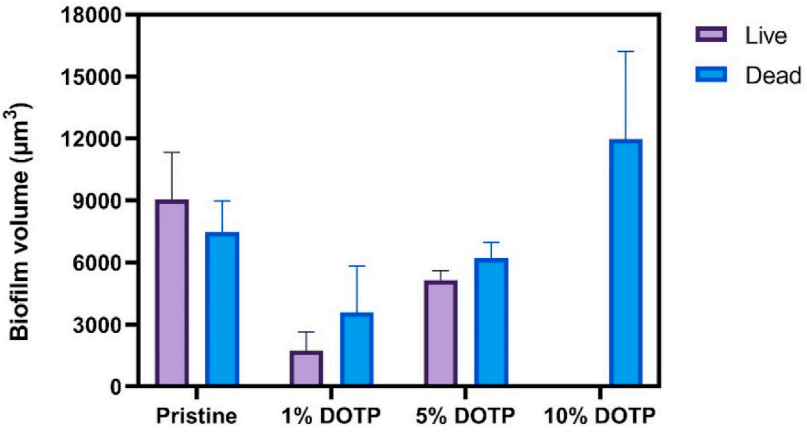
The total biofilm volume increased by approximately 73% from 1% to 5% DOTP, and further increased by approximately 369% from 5% to 10% DOTP. Based on our study, it appears that the initial growth of the biofilm could have been stimulated by increased oxidative stress. Over time, it is possible that a greater amount of DOTP is gradually leaching out of the PVC film and becoming accessible to the biofilm. Determining the precise amount of DOTP that leaches out and its accessibility to biofilms would necessitate specific studies. The excessive concentrations of DOTP might have been toxic to the biofilm, leading to its substantial decay. This can be related to the ROS's hormetic effect on microbial development, where larger amounts harm microorganisms by interfering with essential biological components. Lower ROS concentrations encourage signal transduction and alter metabolic pathways, promoting higher microbial proliferation and the generation of more robust biofilms (Wang et al., 2022).

3.4. Oxidative stress of R. ruber in DOTP-infused PVC film

Oxidative stress, characterized by high levels of ROS inside cells, can cause damage to lipids, proteins, and nucleic acids (Schieber and Chandel, 2014). Previous research has demonstrated that microplastics can trigger the generation of ROS, leading to a decline in cell viability (Wei et al., 2019; Tang et al., 2022). Oxidative stressed cells are indicated by CellROX™ Green which only works when cells are alive. ROS are produced as secondary products during different metabolic processes occurring in viable cells, such as mitochondrial respiration and other cellular pathways. In contrast, deceased cells or cells with impaired metabolism do not generate ROS, resulting in the absence of a fluorescence signal (Lozoya-Gloria et al., 2017). As shown in Fig. 3, no live cells were present when the PVC film containing a volume fraction of 10% v/v DOTP was grown and therefore excluded from the toxicity study. Oxidative stress study revealed that in a lower volume fraction of DOTP (1% v/v), the biofilm volume (Fig. 4b) was close to the biofilm volume on pristine PVC (Fig. 4a). Even with the lowest volume fraction (1% v/v) of DOTP, oxidative stressed cells could be seen in the biofilm. The biofilm's overall volume increased in proportion to the volume fraction of DOTP present in the PVC films. PVC films with 1% DOTP exhibited a biovolume that was 34% higher than pristine PVC, while PVC films with 5% DOTP showed a biovolume increase of 126% compared to PVC with 1% DOTP. As shown in Fig. 4c with 5% DOTP and there seems to be a change in the shape of the bacteria at this concentration. *Rhodococcus* sp. has the ability to undergo morphological changes in response to different stressors like limited nutrients, temperature fluctuations, exposure to toxins, and other adverse conditions as part of their adaptive response (Wang et al., 2020). This type of formation was also observed when we analyzed our samples using FE SEM (Fig. S3, Supplementary Material). Simultaneously, the biovolume of the stressed cells exhibited a substantial increase, showing a 187% greater increment for PVC films with 1% DOTP compared to the pristine PVC. Additionally, a significant 56% rise in biovolume was observed as the DOTP concentration increased from 1% to 5% within the PVC films, in comparison to the biovolume of PVC films containing 1% DOTP. This was quantified with biofilmQ and plotted using 4D XYZC-Scatterplot to display oxidative stressed cells (Fig. 4d–f) and unstressed cells (Fig. 4g–i). The centroid coordinates of the X, Y, and Z axes are shown. The X-axis represents the centroid coordinate x, which indicates the position of each individual cell in the biofilm along the horizontal direction. The Y-axis represents the centroid coordinate y, indicating the position along the vertical direction. The Z-axis represents the centroid coordinate z, which indicates the position of the cell along the depth or axial direction in the biofilm. The coordinates (x, y, and z) are presented in voxel units, which are three-dimensional pixels that define the resolution of the biofilm sample. Each voxel corresponds to a discrete volume element within the biofilm, allowing researchers to precisely locate and analyze individual cells in the three-dimensional biofilm structure. The color-code (C) in the scatterplot represents the cube volume fraction. The cube volume fraction (A_{cube}/A_0) is a measure of how much space in the biofilm is occupied by individual cells (A_{cube}) compared to the total available space (A_0). It provides information about the packing density or occupancy of cells within the biofilm. The higher the cube volume fraction, the more densely packed the cells are in that region of the biofilm. On the surface of the pristine PVC film, there were relatively few stressed cells (Fig. 4a). In contrast, there was a greater abundance of unstressed cells, as shown in (Fig. 4 g). With PVC film that contains the lowest volume fraction of (1% v/v) DOTP present the amount of oxidative stressed cells increased (Fig. 4e) and the amount of unstressed cells was found to be less than that of stressed cells (Fig. 4h). In PVC with the volume fraction of 5 % v/v DOTP, there was an even higher amount of oxidative stressed cells on the surface of the PVC film (Fig. 4f) and overall, there were less unstressed cells present (Fig. 4i). The addition of DOTP to PVC film appears to affect the stress levels of cells on the film's surface. It appears that as the volume fraction of DOTP increases, so does the number of oxidatively stressed cells on the surface. While ROS production is a signaling pathway that can promote biofilm development at lower concentrations, excessive ROS levels may have a toxic effect on microbial viability. Thus, the observed correlation between the concentration of DOTP, ROS production, and biofilm formation underscores the complex relationship between plasticizer content and the



(a) Pristine PVC (b) PVC with 1% DOTP (c) PVC with 5% DOTP (d) PVC with 10% DOTP



(e) Biofilm volume of live and dead cells on the surface of PVC film at different concentrations (pristine, 1%, 5%, and 10%)

Fig. 3. (a–d) Growth of *R. ruber* on PVC film with varying mass fractions (v/v) of DOTP **(ee)** The biofilm volume (μm^3) of live and dead cells on the surface of PVC samples was quantified using BiofilmQ software. The bars depict the mean values derived from triplicate biofilm samples, while the error bars indicate the standard deviations. (For interpretation of the references to color in this figure legend, the reader is referred to the Web version of this article.)

physiological responses of *R. ruber* in the context of PVC films. Further research into the mechanisms by which DOTP influences cell stress levels may be required to gain a deeper understanding of these observations.

3.5. Environmental implication

The findings of this study shed light on the potential impacts of DOTP on microbial communities and ecological processes in soil and water environments. The research indicates that DOTP has the capacity to significantly impact the composition and diversity of microbial communities, thereby altering the overall ecological functions and services provided by these microorganisms. Moreover, exposure to DOTP can lead to the induction of oxidative stress and DNA damage in plastisphere microbes, ultimately affecting their metabolic activities and ability to biodegrade substances. These findings underscore the potential risks associated with DOTP exposure. Although DOTP may be degraded readily under toxic environment (Tran et al., 2021), its degradation rate should be limited if it is embedded in PVC matrix. Because microplastics are environmentally persistent and may carry their hydrophobic additives for long time owing to high partitioning constants between microplastics and water and low leaching rate constants, microplastics can be persistent sources of their additives (Kwon et al., 2017; Do et al., 2022). Additionally, DOTP has the potential to disrupt interactions between plastisphere microbes and other aquatic organisms, including processes such as biofilm formation, nutrient cycling, and trophic transfer. This highlights the potential influence of DOTP on the ecological dynamics and functioning of aquatic ecosystems. Consequently, further research is warranted to deepen our understanding of the ecological implications of DOTP exposure and to develop effective strategies for mitigating its potential adverse effects on microbial communities and ecosystem processes.

4. Conclusion

This study represents the first exploration of the biodegradation pathway of DOTP using a plastic-degrading bacterium. It was found that DOTP can undergo hydrolysis when interacting with biodegrading microbes, producing breakdown products. Remarkably, these products were detected even without an additional carbon source, implying potential biodegradation by *R. ruber*. Higher DOTP concentrations in PVC microplastics correlated with more dead cells and increased ROS production, indicating adverse effects on the plastisphere community. While non-phthalate plasticizers like DOTP were initially considered safer alternatives, this study highlights the importance of understanding their potential impact on microbes. Although DOTP is found in concentrations between 0.6 and 20% in most products, these findings suggest that concentrations of DOTP exceeding 5% may compromise its viability, and even at lower concentrations like 1%, signs of stress were observed. These findings underscore the need for future research on DOTP and its influence on primary colonizers of plastics in aqueous systems (diatoms, cyanobacteria, proteobacteria etc.), biodegradation pathway, and their long-term effects on the environment.

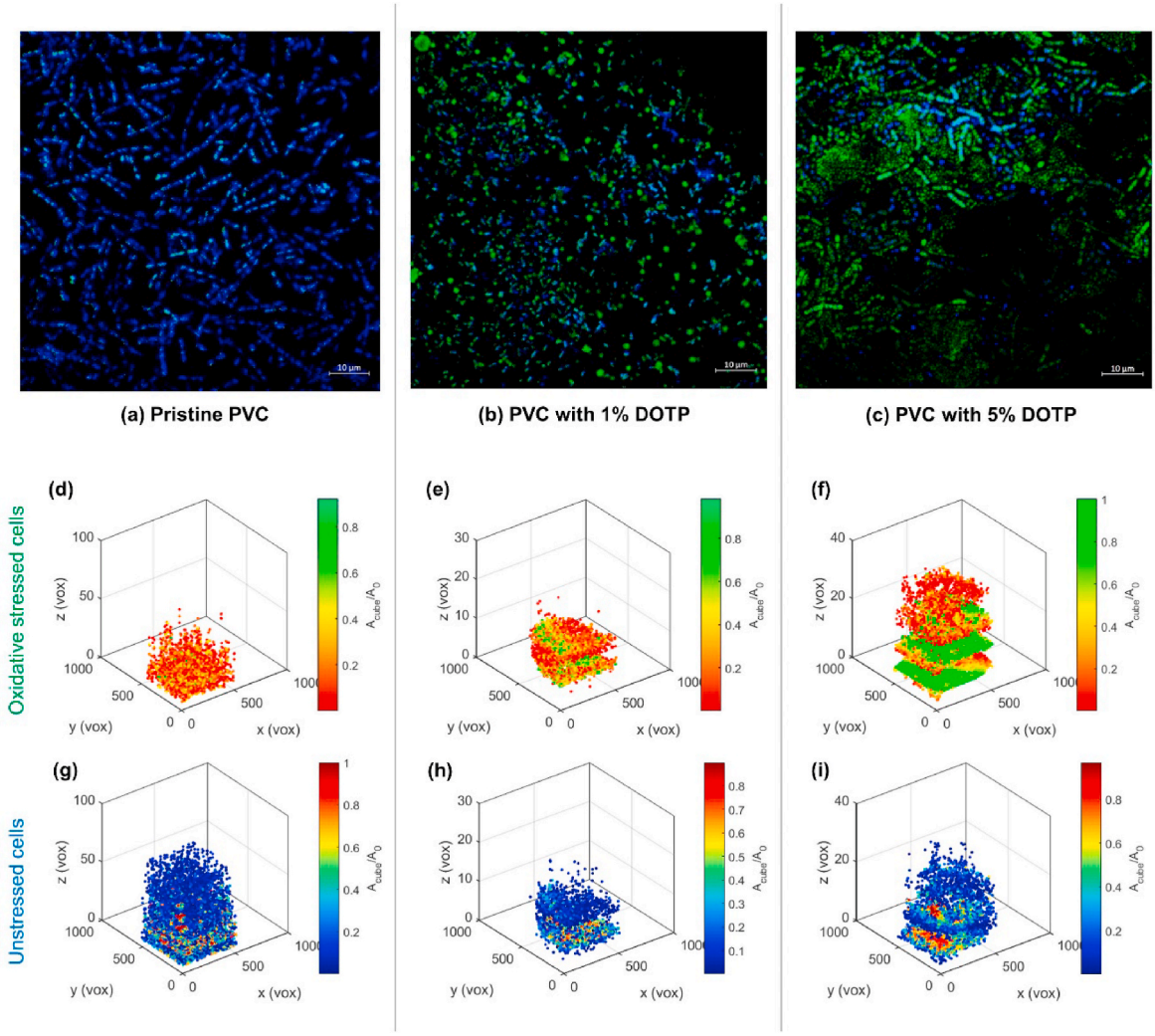


Fig. 4. Blue fluorescence (Hoechst 33342) indicates un-stressed cells and green fluorescence (CellROX™) indicates oxidative stressed cells. **(a–c)** 5 days growth of *R. ruber* on pristine PVC, PVC with 1% (v/v) DOTP, and PVC with 5% (v/v) DOTP respectively. **(d–f)** Oxidative stressed cells are shown in a 4D XYZC-Scatterplot in pristine PVC, PVC with 1% and with 5% (v/v) DOTP respectively. **(g–i)** 4D XYZC-Scatterplot for unstressed cells in the same order as mentioned previously. The X, Y, and Z axes represent the cell's positions in horizontal, vertical, and depth directions, respectively. The coordinates are in voxel units, discrete volume elements for precise analysis. The color-code represents the cube volume fraction. The cube volume fraction (A_{cube}/A_0) is a measure of how much space in the biofilm is occupied by individual cells (A_{cube}) compared to the total available space (A_0). It provides information about the packing density or occupancy of cells within the biofilm. The higher the cube volume fraction, the more densely packed the cells are in that region of the biofilm. (For interpretation of the references to color in this figure legend, the reader is referred to the Web version of this article.)

CRediT authorship contribution statement

Dana Fahad M.S. Mohamed: Writing – original draft, Methodology, Investigation, Data curation, Conceptualization. **Abhrajyoti Tarafdar:** Writing – review & editing, Methodology, Conceptualization. **So Yeon Lee:** Writing – original draft, Investigation, Data curation. **Han Bin Oh:** Writing – review & editing, Supervision, Methodology, Conceptualization. **Jung-Hwan Kwon:** Writing – review & editing, Supervision, Funding acquisition, Conceptualization.

Declaration of competing interest

The authors declare the following financial interests/personal relationships which may be considered as potential competing interests: Jung-Hwan Kwon reports financial support was provided by National Research Foundation of Korea.

Data availability

Data will be made available on request.

Acknowledgments

This work was supported by a National Research Foundation of Korea (NRF) grant funded by the Korean Government (Ministry of Science and ICT) (No. RS-2023-00209242).

Appendix A. Supplementary data

Supplementary data to this article can be found online at https://doi.org/10.1016/j.envpol.2024.124217.

References

Ahmad, H.A., Ahmad, S., Cui, Q., Wang, Z., Wei, H., Chen, X., Ni, S.Q., Ismail, S., Awad, H.M., Tawfik, A., 2022. The environmental distribution and removal of emerging pollutants, highlighting the importance of using microbes as a potential

degrader: a review. Sci. Total Environ. 809, 151926 https://doi.org/10.1016/j.scitotenv.2021.151926.
Aurisano, N.O., Huang, L., Miì, A.I., Canals, L., Jolliet, O., Fantke, P., 2021. Chemicals of concern in plastic toys. Environ. Int. 146, 106194 https://doi.org/10.1016/j.envint.2020.106194.
Auta, H.S., 2017. Bioremediation of Microplastic Using Microbes Isolated from Mangroves Sediments. Faculty of Science.
Beach, E.S., Weeks, B.R., Stern, R., Anastas, P.T., 2013. Plastics additives and green chemistry. Pure Appl. Chem. 85, 1611–1624. https://doi.org/10.1351/PAC-CON-12-08-08/MACHINEREADABLECITATION/RIS.
Bodaghi, A., 2019. An overview on the recent developments in reactive plasticizers in polymers. https://doi.org/10.1002/pat.4790.
Bolívar-Subirats, G., Rivetti, C., Cortina-Puig, M., Barata, C., Lacorte, S., 2021. Occurrence, toxicity and risk assessment of plastic additives in Besos river, Spain. Chemosphere 263, 128022. https://doi.org/10.1016/J.CHEMOSPHERE.2020.128022.
Boor, B.E., Liang, Y., Crain, N.E., Järnström, H., Novoselac, A., Xu, Y., 2015. Identification of phthalate and alternative plasticizers, flame retardants, and unreacted isocyanates in infant crib mattress covers and foam. Environ. Sci. Technol. Lett. 2, 89–94. https://doi.org/10.1021/acs.estlett.5b00039.
Cartwright, C.D., Thompson, I.P., Burns, R.G., 2000. Degradation and impact of phthalate plasticizers on soil microbial communities. Environ. Toxicol. Chem. 19, 1253–1261. https://doi.org/10.1002/ETC.5620190506.
Chiellini, F., Ferri, M., Morelli, A., Dipaola, L., Latini, G., 2013. Perspectives on alternatives to phthalate plasticized poly(vinyl chloride) in medical devices applications. Prog. Polym. Sci. 38, 1067–1088. https://doi.org/10.1016/J.PROGPOLYMSCI.2013.03.001.
Darbre, P.D., 2020. Chemical components of plastics as endocrine disruptors: overview and commentary. Birth Defects Res. 112, 1300–1307. https://doi.org/10.1002/BDR2.1778.
Decho, A.W., Norman, R.S., Visscher, P.T., 2010. Quorum sensing in natural environments: emerging views from microbial mats. Trends Microbiol. 18, 73–80. https://doi.org/10.1016/J.TIM.2009.12.008.
Do, A.T.N., Ha, Y., Kwon, J.H., 2022. Leaching of microplastic-associated additives in aquatic environments: a critical review. Environ. Pollut. 305, 119258 https://doi.org/10.1016/J.ENVPOL.2022.119258.
Eichler, C.M.A., Cohen Hubal, E.A., Little, J.C., 2019. Assessing human exposure to chemicals in materials, products and articles: the international risk management landscape for phthalates. Environ. Sci. Technol. 53, 13583–13597. https://doi.org/10.1021/acs.est.9b03794.
Ghatge, S., Yang, Y., Ahn, J.H., Hur, H.G., 2020. Biodegradation of polyethylene: a brief review. Appl. Biol. Chem. 63, 27. https://doi.org/10.1186/s13765-020-00511-3.
Gilan, I., Sivan, A., 2013. Extracellular DNA plays an important structural role in the biofilm of the plastic degrading actinomycete *Rhodo-coccus ruber*. Adv. Microbiol. 3 https://doi.org/10.4236/aim.2013.38073.
Goudriaan, M., Morales, V.H., van der Meer, M.T.J., Mets, A., Ndhlovu, R.T., van Heerwaarden, J., Simon, S., Heuer, V.B., Hinrichs, K.U., Niemann, H., 2023. A stable isotope assay with 13C-labeled polyethylene to investigate plastic mineralization mediated by Rhodococcus ruber. Mar. Pollut. Bull. 186, 114369 https://doi.org/10.1016/j.marpolbul.2022.114369.
Guevara, G., Castillo Lopez, M., Alonso, S., Perera, J., Navarro-Llorens, J.M., 2019. New insights into the genome of *Rhodococcus ruber* strain Chol-4. BMC Genom. 20, 332. https://doi.org/10.1186/s12864-019-5677-2.
Harmon, J.P., Otter, R., 2018. Green chemistry and the search for new plasticizers. ACS Sustain. Chem. Eng. 6, 2078–2085. https://doi.org/10.1021/acssuschemeng.7b03508.
Harmon, P., Otter, R., 2022. A review of common non-ortho-phthalate plasticizers for use in food contact materials. Food Chem. Toxicol. 164, 112984 https://doi.org/10.1016/j.fct.2022.112984.
Hong, Y., Zeng, J., Wang, X., Drlica, K., Zhao, X., 2019. Post-stress bacterial cell death mediated by reactive oxygen species. Proc. Natl. Acad. Sci. U. S. A. 116, 10064–10071. https://doi.org/10.1073/PNAS.1901730116.
Horn, O., Nalli, S., Cooper, D., Nicell, J., 2004. Plasticizer metabolites in the environment. Water Res. 38, 3693–3698. https://doi.org/10.1016/j.watres.2004.06.012.
Imlay, J.A., 2013. The molecular mechanisms and physiological consequences of oxidative stress: lessons from a model bacterium. Nat. Rev. Microbiol. 11, 443–454. https://doi.org/10.1038/nrmicro3032.
Jebara, A., Albergamo, A., Rando, R., Potortì, A.G., Lo Turco, V., Mansour, H.B., Di Bella, G., 2021. Phthalates and non-phthalate plasticizers in Tunisian marine samples: occurrence, spatial distribution and seasonal variation. Mar. Pollut. Bull. 163, 111967.
Kim, D.Y., Chun, S.-H., Jung, Y., Mohamed, D.F.M.S., Kim, H.-S., Kang, D.-Y., An, J.-W., Park, S.-Y., Kwon, H.-W., Kwon, J.-H., 2020. Phthalate plasticizers in children's products and estimation of exposure: importance of migration rate. Int. J. Environ. Res. Publ. Health 17, 8582. https://doi.org/10.3390/ijerph17228582.
Kim, D.Y., Sochichiu, S., Kwon, J.H., 2022. Effects of time, temperature, and sebum layer on migration rate of plasticizers in polyvinyl chloride products. Chemosphere 308, 136478. https://doi.org/10.1016/j.chemosphere.2022.136478.
Kim, S., Kim, Y., Moon, H.-B., 2021. Contamination and historical trends of legacy and emerging plasticizers in sediment from highly industrialized bays of Korea. Sci. Total Environ. 765, 142751.
Krauskopf, L.G., 2003. How about alternatives to phthalate plasticizers? J Vinyl Additive. Technol. 9, 159–171. https://doi.org/10.1002/vnl.10079.
Krivoruchko, A.V., Iziumova, A.Y., Kuyukina, M.S., Plekhov, O.A., Naimark, O.B., Ivshina, I.B., 2018. Adhesion of *Rhodococcus ruber* IEGM 342 to polystyrene studied using contact and non-contact temperature measurement techniques. Appl. Microbiol. Biotechnol. 102, 8525–8536. https://doi.org/10.1007/s00253-018-9297-6.
Kumar, P., 2018. Role of plastics on human health. Indian J. Pediatr. 85, 384–389. https://doi.org/10.1007/S12098-017-2595-7/TABLES/1.
Kwon, J.H., Chang, S., Hong, S.H., Shim, W.J., 2017. Microplastics as a vector of hydrophobic contaminants: importance of hydrophobic additives. Integrated Environ. Assess. Manag. 13, 494–499. https://doi.org/10.1002/IEAM.1906.
Latini, G., Ferri, M., Chiellini, F., 2010. Materials degradation in PVC medical devices, DEHP leaching and neonatal outcomes. Curr. Med. Chem. 17, 2979–2989. https://doi.org/10.2174/092986710792064992.
Lee, Y.-S., Lim, J.-E., Lee, S., Moon, H.-B., 2020. Phthalates and non-phthalate plasticizers in sediment from Korean coastal waters: occurrence, spatial distribution, and ecological risks. Mar. Pollut. Bull. 154, 111119.
Lorenzetti, S., Benfenati, E., Cozzini, P., Dellafiora, L., Fiorino, F., Ginex, T., Giulivo, M., La Fauci, P., Basile, L., Marcoccia, D., Perissutti, E., Roncaglioni, A., Mantovani, A., 2015. A LIFE-EDESIA project update: an animal-free approach to search for SVHC alternatives. Reprod. Toxicol. 56, 26. https://doi.org/10.1016/j.reprotox.2015.07.058.
Lozoya-Gloria, E., Cornejo-Corona, I., Thapa, H.R., Browne, D.R., Devarenne, T.P., 2017. ROS Detection in *Botryococcus Braunii* Colonies with CellROX Green Reagent, vol. 7, e2508. https://doi.org/10.21769/BioProtoc.2508.
Luo, H., Liu, C., He, D., Sun, J., Li, J., Pan, X., 2022. Effects of aging on environmental behavior of plastic additives: migration, leaching, and ecotoxicity. Sci. Total Environ. 849, 157951 https://doi.org/10.1016/J.SCITOTENV.2022.157951.
Meeker, J.D., Sathyanarayana, S., Swan, S.H., 2009. Phthalates and other additives in plastics: human exposure and associated health outcomes. Phil Trans R Soc B 364, 2097–2113. https://doi.org/10.1098/RSTB.2008.0268.
Mor, R., Sivan, A., 2008. Biofilm formation and partial biodegradation of polystyrene by the actinomycete Rhodococcus ruber: biodegradation of polystyrene. Biodegradation 19, 851–858. https://doi.org/10.1007/s10532-008-9188-0.
Morris, J.J., Rose, A.L., Lu, Z., 2022. Reactive oxygen species in the world ocean and their impacts on marine ecosystems. Redox Biol. 52, 102285.
Mukherjee, S., Bassler, B.L., 2019. Bacterial quorum sensing in complex and dynamically changing environments. Nature Rev. Microbiology 2019 17, 371–382. https://doi.org/10.1038/s41579-019-0186-5.
Nalli, S., Cooper, D.G., Nicell, J.A., 2002. Biodegradation of plasticizers by Rhodococcus rhodochrous. Biodegradation 13, 343–352. https://doi.org/10.1023/A:1022313810852.
Naloka, K., Jaroonrunganan, J., Woratecha, N., Khondee, N., Nojiri, H., Pinyakong, O., 2022. Physiological changes in Rhodococcus ruber S103 immobilized on biobooms using low-cost media enhance stress tolerance and crude oil-degrading activity. Sci. Rep. 12, 10474 https://doi.org/10.1038/s41598-022-14488-0.
Pathak, V.M., Navneet, 2017. Review on the current status of polymer degradation: a microbial approach. Bioresour Bioprocess 4, 15. https://doi.org/10.1186/s40643-017-0145-9.
Pérez-Albaladejo, E., Solé, M., Porte, C., 2020. Plastics and plastic additives as inducers of oxidative stress. Curr. Opin. Toxicol. 20–21, 69–76. https://doi.org/10.1016/J.COTOX.2020.07.002.
Rais-Bahrami, K., Revenis, M.E., Short, B.L., Nunez, S., Luban, N.L.C., 2004. Adolescents exposed to DEHP in plastic tubing as neonates: research briefs. Pediatr. Nurs. 30, 406–408.
Schieber, M., Chandel, N.S., 2014. ROS function in redox signaling and oxidative stress. Curr. Biol. 24, R453–R462. https://doi.org/10.1016/J.CUB.2014.03.034.
Seixas, A.F., Quendera, A.P., Sousa, J.P., Silva, A.F.Q., Arraiano, C.M., Andrade, J.M., 2021. Bacterial response to oxidative stress and RNA oxidation. Front. Genet. 12 https://doi.org/10.3389/FGENE.2021.821535.
Shah, D., Burgess, J., 2009. One-minute method for the screening of phthalates in toys at regulatory limits using UPLC/MS and empower software. WATERS application note 1–6.
Sharma, H., Neelam, D.K., 2023. Understanding challenges associated with plastic and bacterial approach toward plastic degradation. J. Basic Microbiol. 63, 292–307. https://doi.org/10.1002/jobm.202200428.
Tang, M., Zhou, S., Huang, J., Sun, L., Lu, H., 2022. Stress responses of sulfate-reducing bacteria sludge upon exposure to polyethylene microplastics. Water Res. 220, 118646.
Tarafdar, A., Lee, J.U., Jeong, J.E., Lee, H., Jung, Y., Oh, H. Bin, Woo, H.Y., Kwon, J.H., 2021. Biofilm development of *Bacillus siamensis* ATKU1 on pristine short chain low-density polyethylene: a case study on microbe-microplastics interaction. J. Hazard Mater. 409, 124516 https://doi.org/10.1016/J.JHAZMAT.2020.124516.
Tarafdar, A., Lim, J. yun, Kwon, J.H., 2022. UV stabilizers can foster early development of biofilms on freshwater microplastics. Environ. Pollut. 315, 120444 https://doi.org/10.1016/J.ENVPOL.2022.120444.
Tarafdar, A., Mohamed, D.F.M.S., Kwon, J.H., 2023. Marine microplastics: abundance, ecotoxic consequences of associated anthropogenic contaminants and interactions with microorganisms. Energy, Environment, and Sustainability 11–46. https://doi.org/10.1007/978-981-99-2062-4_2/COVER.
Tran, H.T., Lin, C., Bui, X.T., Itayama, T., Dang, B.T., Cheruiyot, N.K., Hoang, H.G., Vu, C.T., 2021. Bacterial community progression during food waste composting containing high dioctyl terephthalate (DOTP) concentration. Chemosphere 265, 129064. https://doi.org/10.1016/J.CHEMOSPHERE.2020.129064.
Tüzüm Demir, A.P., Ulutan, S., 2015. Degradation kinetics of PVC plasticized with different plasticizers under isothermal conditions. J. Appl. Polym. Sci. 132, 41579 https://doi.org/10.1002/app.41579.

Tüzüm Demir, A.P., Ulutan, S., 2013. Migration of phthalate and non-phthalate plasticizers out of plasticized PVC films into air. J. Appl. Polym. Sci. 128, 1948–1961. https://doi.org/10.1002/app.38291.

Unterberg, H., Weidenhaupt, H.J., Wiedemeier, M., 2011. Changes in environmental legislation boost demand for ecologically sound products. Chem. Listy 105, s258–s259.

Vikhareva, I.N., Aminova, G.K., Mazitova, A.K., 2021. Ecotoxicity of the adipate plasticizers: influence of the structure of the alcohol substituent. Molecules 26, 4833. https://doi.org/10.3390/MOLECULES26164833.

Wang, C., Chen, Y., Zhou, H., Li, X., Tan, Z., 2020. Adaptation mechanisms of Rhodococcus sp. CNS16 under different temperature gradients: physiological and transcriptome. Chemosphere 238, 124571. https://doi.org/10.1016/J.CHEMOSPHERE.2019.124571.

Wang, H., Yu, P., Schwarz, C., Zhang, B., Huo, L., Shi, B., Alvarez, P.J.J., 2022. Phthalate esters released from plastics promote biofilm formation and chlorine resistance. Environ. Sci. Technol. 56, 1081–1090. https://doi.org/10.1021/acs.est.1c04857.

Wang, Q., De Oliveira, E.F., Alborzi, S., Bastarrachea, L.J., Tikekar, R.V., 2017. On mechanism behind UV-A light enhanced antibacterial activity of gallic acid and propyl gallate against Escherichia coli O157:H7. Sci. Rep. 7, 1–11. https://doi.org/10.1038/s41598-017-08449-1.

Wei, W., Huang, Q.-S., Sun, J., Dai, X., Ni, B.-J., 2019. Revealing the mechanisms of polyethylene microplastics affecting anaerobic digestion of waste activated sludge. Environ. Sci. Technol. 53, 9604–9613.

Wright, R.J., Bosch, R., Gibson, M.I., Christie-Oleza, J.A., 2020. Plasticizer degradation by marine bacterial isolates: a proteogenomic and Metabolomic Characterization. Environ. Sci. Technol. 54, 2244–2256.

Xie, M., Wu, Y., Little, J.C., Marr, L.C., 2016. Phthalates and alternative plasticizers and potential for contact exposure from children's backpacks and toys. J. Expo. Sci. Environ. Epidemiol. 26, 119–124. https://doi.org/10.1038/jes.2015.71.

Yang, T., Ren, L., Jia, Y., Fan, S., Wang, Junhuan, Wang, Jiayi, Nahurira, R., Wang, H., Yan, Y., 2018. Biodegradation of di-(2-ethylhexyl) phthalate by *Rhodococcus ruber* YC-YT1 in contaminated water and soil. Int J Environ Res Public Health 15, 964. https://doi.org/10.3390/IJERPH15050964.

Yousif, E., Ahmed, A., Abood, R., Jaber, N., Noaman, R., Yusop, R., 2015. Poly(vinyl chloride) derivatives as stabilizers against photodegradation. J. Taibah Univ. Sci. 9, 203–212. https://doi.org/10.1016/J.JTUSCI.2014.10.003.

Zhao, X., Drlica, K., 2014. Reactive oxygen species and the bacterial response to lethal stress. Curr. Opin. Microbiol. 1–6. https://doi.org/10.1016/j.mib.2014.06.008, 0.